PHYSICAL REVIEW D **76,** 115009 (2007)

Towards realistic standard model from D-brane configurations

G. K. Leontaris,[1] N. D. Tracas,[2] N. D. Vlachos,[3] and O. Korakianitis[2]

[1]*Theoretical Physics Division, Ioannina University, GR 451 10 Ioannina, Greece*

[2]*Physics Department, National Technical University, GR 157 73 Athens, Greece*

[3]*Department of Theoretical Physics, Aristotle University of Thessaloniki, GR 541 24 Thessaloniki, Greece*

(Received 5 September 2007; published 12 December 2007)

Effective low energy models arising in the context of D-brane configurations with standard model (SM) gauge symmetry extended by several gauged Abelian factors are discussed. The models are classified according to their hypercharge embeddings consistent with the SM spectrum hypercharge assignment. Particular cases are analyzed according to their perspectives and viability as low energy effective field theory candidates. The resulting string scale is determined by means of a two-loop renormalization group calculation. Their implications in Yukawa couplings, neutrinos and flavor changing processes are also presented.

DOI: 10.1103/PhysRevD.76.115009 PACS numbers: 11.25.Wx, 11.10.Hi, 11.30.Pb, 12.60.Jv

I. INTRODUCTION

The revelation of the higher dimensional objects [1], called D-branes, has revived the interest on model building in the context of string theory. As a consequence, during the last decade, numerous painstaking efforts have been devoted to the study of possible D-brane realizations of the standard model and the higher gauge symmetries containing it.[1]

Model building in string theory has shown that there is no *a priori* obvious recipe to obtain the SM from the first principles of the theory. In recent attempts, various groups [3–11] started mainly a bottom-up approach delving into the string vacua, aiming to systematically classify all possible D-brane configurations, seeking an acceptable effective low energy theory which reproduces the success of the standard model. It is anticipated that such a construction would determine the arbitrary parameters of the standard model, while new phenomena could be predicted and eventually tested in future experiments.

In the present work, we elaborate on low energy implications of a particular class of D-brane models [4–11] with standard model gauge symmetry and split-supersymmetric spectrum [12].[2] The implementation of split supersymmetry in the D-brane constructions under consideration is justified for the following two reasons: First, it was shown that the realization of split SUSY is a viable possibility in certain D-brane constructions [14]. Second, intermediate and high string scale D-brane models previously abandoned because of phenomenological drawbacks related to hierarchy problems, rapid proton decay, etc., in the context of split supersymmetry offer fascinating new possibilities since there exist now convincing arguments concerning the hierarchy issues. Besides, the renormalization group flow of the gauge and Yukawa couplings as well as low energy measurable physical quantities dependent on them, change substantially. In view of these interesting novelties, in a previous work [6], a classification of the various D-brane derived models with split-supersymmetric spectrum and standard model gauge symmetry extended by $U(1)$ factors was attempted. All possible configurations with $P = 1, 2, 3$ Abelian branes were considered and the different hypercharge embeddings compatible with the SM particle spectrum were found. In all viable cases, a one-loop renormalization-group (RG) analysis was used to calculate the string scale M_S, while the fermion mass relations of the third generation, the gaugino masses, and the lifetime of the gluino were examined. Here, we will pursue a further investigation, addressing more phenomenological issues and deriving possible constraints on the split supersymmetry breaking scale $\tilde{m}$ and other so far undetermined parameters. We will extend our previous analysis, and work out in detail the predictions for the string scale using renormalization group equations at two-loop order. We note however, that the determination of the string scale is more intricate than in ordinary grand unified models. The reason is that in D-brane constructions, gauge coupling unification at the string scale does not occur since the volume of the internal space is involved between gauge and string couplings; thus, the actual values of the SM gauge coupling constants may differ at M_S. This arbitrariness looks rather daunting; however, certain internal volume relations could allow for partial unification. In order to reduce the number of free parameters and obtain definite predictions, we mainly concentrate on cases where certain relations are assumed to connect the gauge couplings at the string scale. Particular attention is also given to models where the non-Abelian gauge couplings have a common value at M_S. Next, in each case of the models under consideration, we determine the range of the split-supersymmetric scale which is compatible with the chosen gauge coupling conditions. We further discuss the Yukawa potential and other low energy predictions which are crucial for the viability of the models. In particular, we exam-

[1]For a comprehensive and pedagogical introduction see [2,3].

[2]For another approach in partly supersymmetric spectrum see Ref. [13].

ine the conditions under which exotic processes like the lepton flavor violating decay $\mu \to e\gamma$ can be detected in future experiments, we discuss suggested mechanisms predicting a sufficiently heavy mass for the right-handed neutrino and check the existence of exotic matter like leptoquarks, whose appearance is also possible in the low energy spectrum of these models.

The paper is organized as follows: In the next section, we summarize the salient features of the D-brane configurations and determine the hypercharge embeddings leading to standard model particle spectrum. In Sec. III we present in some detail selected cases of low energy effective models, while in Sec. IV we calculate the string scale and explore its correlation with the split-supersymmetric scale by means of a two-loop renormalization group analysis. In Sec. V we analyze the effects of exotic states. In Sec. VI we discuss the observability conditions for rare flavor violation like $\mu \to e\gamma$. Finally, in Sec. VII we present our conclusions.

II. D-BRANE CONFIGURATIONS AND SPLIT SUPERSYMMETRY

The embedding of the standard model in a D-brane configuration as well as some implications in low energy phenomenology and the magnitude of the string scale have been explored in several works [4–8]. The same problem in the context of intersecting D-branes has also been extensively discussed [9,10].

The resulting field theory model involves the SM non-Abelian gauge symmetry extended by several $U(1)$ factors, a linear combination of which defines the hypercharge.[3] A systematic bottom-up investigation of all possible configurations for the SM gauge symmetry with two Abelian branes was presented in [7]. Here, as in [8], we assume the existence of at most three extra $U(1)$ Abelian branes, thus, the full gauge group is

$$G = U(3)_C \times U(2)_L \times U(1)^P, \qquad P = 1, 2, 3. \tag{1}$$

Since $U(n) \sim SU(n) \times U(1)$, the final symmetry is

$$G = SU(3)_C \times SU(2)_L \times U(1)^{P+2}, \qquad P = 1, 2, 3 \tag{2}$$

while the SM fermions and Higgs fields carry additional quantum numbers under the extra $U(1)$'s.

Given that strings attached to various D-brane stacks represent the SM matter fields, the hypercharge generator is, in general, a linear combination of all possible $U(1)$ factors. If we define the anomaly free linear combination of these $U(1)$'s to be

$$Y = k_3 Q_3 + k_2 Q_2 + \sum_{i=1}^{3} k_i' Q_i',$$

the most general hypercharge gauge coupling condition can be written as

$$\frac{1}{g_Y^2} = \frac{6k_3^2}{g_3^2} + \frac{4k_2^2}{g_2^2} + 2\sum_{i=1}^{P} \frac{k_i'^2}{g_i'^2}. \tag{3}$$

For a given hypercharge embedding, the k_i''s can be determined and Eq. (3) relates the weak angle $\sin^2\theta_W = (1 + k_Y)^{-1}$ ($k_Y = \frac{\alpha_2}{\alpha_Y}$, $\alpha_i \equiv g_i^2/4\pi$), with the gauge coupling ratios at the string scale M_S. Since in D-brane scenarios the gauge couplings do not necessarily attain a common value at the string (brane) scale M_S, the ratios α_2/α_3, α_2/α_i' differ from unity there. In a previous analysis, various relations between the gauge couplings were considered and a systematic investigation of the magnitude of the string scale and the split SUSY breaking mass scale was presented [8]. Here, in order to reduce the arbitrary parameters and come up with definite predictions, we assume the existence of relations between the gauge couplings at M_S, while we pay particular attention to the interesting case $\alpha_2 = \alpha_3$ at M_S. If we accept that $m \leq P$ $U(1)$ branes are aligned with the $U(3)$ stack and the remaining $P - m$ Abelian branes are aligned with the $U(2)$ set, k_Y becomes

$$k_Y \equiv \frac{\alpha_2}{\alpha_Y} = n_1\xi + n_2 \tag{4}$$

where

$$n_1 = 6k_3^2 + 2\sum_{i=1}^{m} k_i'^2, \qquad n_2 = 4k_2^2 + 2\sum_{i=m+1}^{P} k_i'^2, \tag{5}$$

and ξ is the ratio of the non-Abelian gauge couplings α_2/α_3.

To obtain the fermion and Higgs spectrum of a given brane configuration, we note that each state corresponds to an open string stretched between pairs of brane stacks or to a string with both ends attached to the same brane stack. Taking all possible arrangements of the SM particle spectrum represented by the various strings attached between the $U(3)$, $U(2)$ and extra $U(1)_i$ brane sets, we end up with the admissible brane configurations. Some particular arrangements are shown in Fig. 1. For each particular configuration, the coefficients $k_{2,3}$, k_i' are determined by the requirement that the SM particle spectrum acquires the correct hypercharge.

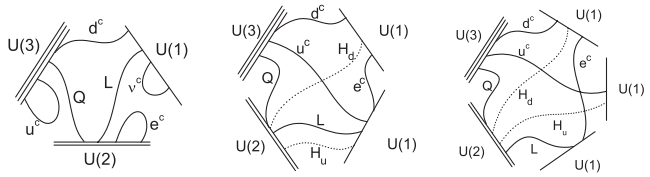

FIG. 1. Selected standard model configurations with one, two, and three Abelian branes $P = 1, 2, 3$.

[3] See reviews [3,11].

TABLE I. Simplest hypercharge embeddings for the $P = 1, 2, 3$ brane configurations. The last column shows the (n_1, n_2) values of (5) for the various possible alignments of the $U(1)$ branes with respect to $U(3)$ and $U(2)$ brane-stack orientations.

P		$\lvert k_3\rvert$	$\lvert k_2\rvert$	$\lvert k_1'\rvert$	$\lvert k_2'\rvert$	$\lvert k_3'\rvert$	(n_1, n_2)
1	a_1	$\frac{1}{3}$	$\frac{1}{2}$	0	-	-	$(\frac{2}{3}, 1)$
	b_1	$\frac{1}{6}$	0	$\frac{1}{2}$	-	-	$(\frac{2}{3}, 0); (\frac{1}{6}, \frac{1}{2})$
2	a_2	$\frac{1}{6}$	0	$\frac{1}{2}$	$\frac{1}{2}$	-	$(\frac{1}{6}, 1); (\frac{7}{6}, 0); (\frac{2}{3}, \frac{1}{2})$
	b_2	$\frac{2}{3}$	$\frac{1}{2}$	1	0	-	$(\frac{8}{3}, 3); (\frac{14}{3}, 1)$
	c_2	$\frac{1}{3}$	$\frac{1}{2}$	0	1	-	$(\frac{2}{3}, 3); (\frac{8}{3}, 1)$
3	a_3	$\frac{1}{6}$	0	$\frac{1}{2}$	$\frac{1}{2}$	$\frac{1}{2}$	$(\frac{1}{6}, \frac{3}{2}); (\frac{2}{3}, 1); (\frac{5}{3}, 0); (\frac{7}{6}, \frac{1}{2})$
	b_3	$\frac{1}{3}$	$\frac{1}{2}$	0	1	1	$(\frac{2}{3}, 5); (\frac{14}{3}, 1); (\frac{8}{3}, 3)$
	c_3	$\frac{2}{3}$	$\frac{1}{2}$	1	0	0	$(\frac{8}{3}, 3); (\frac{14}{3}, 1)$

To proceed further, we recall here the results obtained for brane setups that include up to three Abelian branes. The admissible solutions for the $U(3) \times U(2) \times U(1)$ case setup have been explored in [14] and the k_i distinctive solutions are presented in the first two lines of Table I. For the $U(3) \times U(2) \times U(1)^2$ configuration [4,5,7], we assign the quantum numbers of the SM particles $Q(3, 2; +1, \epsilon_1, 0, 0)$, $d^c(\bar{3}, 1; -1, 0, \epsilon_2, 0)$, $u^c(\bar{3}, 1; -1, 0, 0, -\epsilon_3)$, $L(1, 2; 0, \epsilon_4, 0, \epsilon_5)$, and $e^c(1, 1; 0, 0, \epsilon_6, \epsilon_7)$, where $\epsilon_i = \pm 1$. A similar assignment can be written for the $P = 3$ case too. Solving the corresponding hypercharge assignment equations [6,8], we find that the hypercharge can be expressed in terms of $k_2' = x$ which remains undetermined, as

$$Y = (2/3 - x)Q_3 + (1/2 - x)Q_2 + (1 - x)Q_1' + xQ_2' + \delta_{N3}xQ_3'. \tag{6}$$

Choosing appropriate values for x so that the corresponding boson remains massless at M_S, the simplest solutions for the three different brane configurations are shown in Table I. For future use, the values of the coefficients n_1, n_2 appearing in (5) for all possible $U(3)$ and/or $U(2)$ alignments of the $U(1)$ branes are also included in the last column of the same Table.

III. LOW ENERGY EFFECTIVE MODELS OF PARTICULAR EMBEDDINGS

In the previous section we saw that the SM spectrum can be successfully accommodated in D-brane setups with gauge symmetry of the form $U(3) \times U(2) \times U(1)^P$, $P = 1, 2, 3$, and made a complete classification of models for the various hypercharge embeddings which imply a realistic particle content. In this section, we will present the particular embeddings in more detail, and work out the Yukawa couplings and other phenomenologically interesting features.

In a previous work [8], we presented an analysis dealing with the implications of split supersymmetry on the string scale, first considering models that arise in parallel brane scenarios where the $U(1)$ branes are superposed with the $U(2)$ or $U(3)$ brane stacks. Varying the split SUSY scale in a wide range, we examined the evolution of the gauge couplings and found three distinct classes of models with respect to the string scale. The split supersymmetry breaking scale $\tilde{m}$, can in principle be much larger than the electroweak scale and, as a consequence, squarks and sleptons can obtain large masses of order $\tilde{m}$, while the corresponding fermionic degrees as well as gauginos and higgsinos, remain light. This splitting of the spectrum is made possible only when the dominant source of supersymmetry breaking preserves an R-symmetry which protects fermionic degrees from obtaining masses at the scale $\tilde{m}$.

Assuming that above $\tilde{m}$ only the minimal supersymmetric standard model (MSSM) spectrum exists, while below $\tilde{m}$ we only have SM fermions, gauginos, higgsinos and one linear combination of the scalar Higgs doublets, the one-loop renormalization group equation RGE expression for the string scale is given by

$$M_S = M_Z\left(\frac{\tilde{m}}{M_Z}\right)^a e^b \tag{7}$$

where, the parameters a, b depend on the beta function coefficients, the values of the gauge couplings at M_Z, and the model dependent constants n_1, n_2 given in (5). After substituting the beta functions, these constants are given by

$$a = \frac{21 - 12n_1 - 13n_2}{6(11 + 3n_1 - n_2)}b = \frac{2\pi}{11 + 3n_1 - n_2}\left(\frac{1}{\alpha_Y} - \frac{n_2}{\alpha_2} - \frac{n_1}{\alpha_3}\right).$$

The above one-loop formula is sufficient to produce some qualitative results. Thus, one class of models that arises in the configurations with $P = 1$ and $P = 3$ Abelian branes predicts a string scale of the order of the SUSY grand unified theory scale $M_S \sim 10^{16}$ GeV; interestingly enough, these models also imply that the non-Abelian gauge couplings unify ($\alpha_2 = \alpha_3$) at M_S.

In the case of the configuration with only one Abelian brane, the up or down right-handed quarks arise when both endpoints of an open string are attached to the color stack. In this case, the terms Qu^c or Qd^c carry a nonzero $U(1)_C$ charge while a typical SM Higgs field is not charged under $U(1)_C$. Therefore, the corresponding tree-level Yukawa term is not allowed and the quark fields remain massless. It is worth noting that, as shown by one-loop renormalization group analysis [8], $\tilde{m}$, at least in its minimal SM content, is fixed at a relatively small scale $\sim$6 TeV. The corresponding—with respect to the $M_S \sim 10^{16}$ GeV prediction—$P = 3$ case is free from these shortcomings; consequently, in what follows, we are going to further

elaborate on some interesting low energy implications of this setup.

Another category of brane configurations was found in a particular—with respect to the $U(1)$ alignments—case of the $P = 2$ Abelian branes. This model corresponds to a specific $U(1)$ brane orientation and predicts an intermediate string scale $M_S \sim 10^6$–10^7 GeV. Finally, two more cases in the $P = 2$ and $P = 3$ Abelian brane scenarios result in a low M_S, in the TeV range. In the following, we shall give a detailed description of two promising cases with three and two Abelian branes, respectively.

A. A representative case with $U(3) \times U(2) \times U(1)^3$ gauge symmetry

This model possesses interesting characteristics and enough freedom to produce reliable phenomenology. The hypercharge assignment corresponds to the solution a_3 of Table I. Depending on the orientations of the $U(1)$ branes which are taken to be either parallel to the $U(3)$ or to the $U(2)$ stack, we obtain four distinct cases. In particular, if we align the two $U(1)$ branes with the $U(2)$ stack, we get $k_Y = \frac{1}{6}\xi + \frac{3}{2}$, and one obtains non-Abelian gauge unification $\xi = \frac{\alpha_2}{\alpha_3} = 1$ at a scale $M_S \approx 10^{16}$ GeV. It is worth noting that this particular $U(1)$ brane alignment results in a $U(1)$ normalization constant $k_Y = \frac{5}{3}$ and $\sin^2\theta_w(M_S) = \frac{3}{8}$. These are undeniably interesting attributes reminiscent of the successful grand unified theories, while in addition, a sufficiently large mass for the right-handed neutrino arises to realize the seesaw mechanism. Note also that all other possible $U(1)$ alignments of the $P = 3$ setup lead to a similar unification scale, but with a weak dependence on the $\tilde{m}$ scale. Demanding the existence of appropriate Yukawa couplings, the various signs are fixed and this configuration leads to the charge assignments presented in Table II. The field ν^c, in particular, included in the spectrum is a generic type of singlet which may arise from a string with endpoints attached on two different $U(1)$ branes, thus, the possible values of $s_{i=1,2,3}$ are equal to $0, \pm 1$. Once the two branes where the corresponding string is attached are specified, the values of s_i, can be chosen so that ν^c can be identified with a right-handed neutrino. The hypercharge operator is defined (see Table I) as follows:

$$Y = \tfrac{1}{6}Q_c + \tfrac{1}{2}(Q_1 + Q_1' + Q_1'')\cdot \tag{8}$$

Taking into account the charge assignment of the SM states presented in Table II, we can derive the allowed tree-level Yukawa couplings for the charged fermions which are

$$\lambda_u Q u^c H_u + \lambda_d Q d^c H_d + \lambda_l L e^c H_d\cdot \tag{9}$$

The potential mass terms (9) do not discriminate between generations; therefore, some other mechanism has to be invented in order to generate flavor mixing. This can be achieved in the case of intersecting branes, where quarks and leptons as well as Higgs fields appear at the intersections and are located at different positions in the compact extra dimensions [9,15]. The six-dimensional compact space is usually taken to be a six-dimensional factorizable torus $T^6 = \prod_{i=1}^3 T_i^2$ while strings representing the matter fields are wrapped along the two 1-cycles of each of the three torii. The number of fermion generations is related to the two distinct numbers of brane wrappings around the two circles of the three torii. For example, for a string with endpoints attached on two stacks a, b [corresponding to a $(N_a, \bar{N}_b)$ representation] and wrapping numbers (n_a^i, m_a^i), (n_b^i, m_b^i), the number of intersections $I_{ab} = \prod_{i=1}^3 (n_a^i m_b^i - n_b^i m_a^i)$ equals the number of chiral fermions at the intersection. In this scenario, the trilinear flavor mixing Yukawa couplings of the form $\lambda^{ijk} f_i^c f_j h_k$ arise from a string world sheet stretching between the three relevant brane stacks, while the coupling strengths are of the order $\lambda^{ijk} \sim e^{-A_{ijk}}$, where A_{ijk} is the triangular area generated by the three vertices related to the fermions f_i^c, f_j and the Higgs field h_k. We note, however, that in the present model one might exploit the fact that the three $U(1)$ charges Q_1, Q_1', and Q_1'' appear symmetrically in the hypercharge definition. This allows for the possibility of having open strings with one end attached to a certain non-Abelian stack and the other endpoint attached to a different $U(1)$ brane. In this case, the corresponding SM states have the same $SU(3) \times SU(2) \times U(1)_Y$ quantum numbers, although they are differently charged under the extra $U(1)$'s. The latter could act as a family symmetry distinguishing between the various—"flavor dependent"—Yukawa terms. As an example, assume that in addition to the string representing the u^c of Table II, we also add a string with one end attached to the $U(3)$ stack and the other end to the first $U(1)$ brane with quantum numbers $(\bar{3}, 1; -1, -1, 0, 0, 0)$. This could also be interpreted as a right-handed up-quark field (denoted here as u'^c) belonging to a different family; however, another tree-level term $Q u'^c H_u$ is prevented by the $U(1)$ symmetry. A mass term for this u'^c could be possible in the presence of a neutral scalar singlet $(1, 1; -1, 1, 0)$ [represented by a string with ends on the appropriate $U(1)$ branes] so that a hierarchically suppressed mass term of the form $Q u'^c H_u \frac{\langle\phi\rangle}{M_S}$

TABLE II. The quantum numbers of the SM matter fields for the $N = 3$ brane configuration. The particular choice of signs are fixed by hypercharge and Yukawa couplings constraints.

	$SU(3) \times SU(2)$	Q_3	Q_2	Q_1'	Q_2'	Q_3'
Fermions	$Q(3, 2)$	1	ϵ_1	0	0	0
	$u^c(\bar{3}, 1)$	-1	0	0	-1	0
	$d^c(\bar{3}, 1)$	-1	0	1	0	0
	$L(1, 2)$	0	ϵ_1	0	0	-1
	$e^c(1, 1)$	0	0	1	0	1
	$\nu^c(1, 1)$	0	0	s_1	s_2	s_3
Bosons	$H_u(1, 2)$	0	$-\epsilon_1$	0	1	0
	$H_d(1, 2)$	0	$-\epsilon_1$	-1	0	0

could arise. Similar terms can also be generated for the lepton fields.

Returning now to the minimal version of the present model, it can be easily checked that the Lepton number is identified with the $\mathcal{L} = -Q_3'$ charge of the above states, so that the lepton doublet L and the singlet e^c carry lepton numbers $+1$ and -1, respectively, while all other states are neutral under Q_3'. Taking into account this definition of the Lepton number, we deduce that there are only two possibilities to accommodate the right-handed neutrino. If we choose $s_1 = 0, s_2 = -1, s_3 = +1$, we get a ν^c state with $U(1)$ charges $(0, 0, 0, -1, 1)$ and zero hypercharge. Then a Yukawa coupling of the form

$$\lambda_l L H_u \nu^c \tag{10}$$

is compatible with all $U(1)$ symmetries, providing the neutrino with Dirac mass. This Dirac mass term is naturally of the same order of magnitude as the corresponding mass terms for charged lepton fields. Its suppression down to the present experimental limits is achieved via the seesaw mechanism; therefore, a Majorana neutrino mass term $M_{\nu^c}\nu^c\nu^c$ with $M_{\nu^c} \sim M_S$ is required. Unfortunately, a mass scale of this high order in not possible to get in the perturbative superpotential. A nonperturbative origin for M_{ν^c} and, in particular, from string theory instanton effects was proposed in [16]. According to this approach, the operator

$$M_S e^{-S_{\text{inst.}}} \nu^c \nu^c \tag{11}$$

which provides a Majorana mass to ν^c is found to be gauge invariant, while it violates the $B - L$ symmetry. The relevant instantons correspond to D2-branes which, when intersecting with D6-brane stacks give rise to fermionic zero modes charged under particular $U(1)$'s. An instanton induced effective interaction is generated by integrating over the instanton zero modes. Fermion zero modes charged under the particular $U(1)$ violate the corresponding $U(1)$ symmetry; therefore, it is necessary to insert fields charged under the 4d symmetry. In the case under consideration, a D2-brane when intersecting with the two D6 branes, where the string representing ν^c is attached, gives rise to a Majorana mass term of the form (11), thus the seesaw mechanism is operative in this model.

It has been observed [7,17] that in addition to the SM particle spectrum discussed above, in several D-brane constructions, states which carry both lepton and quark quantum numbers are unavoidable. Indeed, fields of the type $D, U = (3/\bar{3}, 1)_{(\pm 1,0,0,0,1)}$ and their complex conjugates obtained by strings attached on $U(3)$ and the corresponding $U(1)$ stacks are also possible. These representations have the quantum numbers of leptoquarks, i.e., they are color triplets and carry lepton number $\mathcal{L} = \pm 1$. Fortunately, couplings of the form $\bar{D}QL$ and $Du^c e^c$ that might lead to baryon instability are not allowed because of $U(1)$ symmetries. Nevertheless, these states do contribute to the beta function coefficients and thus can have a significant impact on the determination of the string and split SUSY scales. In the following sections, a more general analysis that will also include leptoquarks will be presented.

B. A case with $U(3) \times U(2) \times U(1)^2$ gauge symmetry and low M_S

We will now describe a model which admits a low unification scale.[4] We consider the case b_2 of Table I where both $U(1)$ branes are aligned to the $U(3)$ stack. A rough estimate of the unification scale at one-loop order gives $M_S \sim 10^5 \times (m_Z/\tilde{m})^{1/3}$, and it can be checked (7) that its highest value cannot exceed 10^5 GeV.

The hypercharge assignments of the SM states $Q(3, 1; 1, -1, 0, 0)$, $u^c(\bar{3}, 1; -1, 0, 0, \epsilon_3)$, $d^c(\bar{3}, -1, 0, 1, 0)$, $L(1, 2; 0, -1, 0, \epsilon_5)$, and $e^c(1, 1; 0, 0, 1, \epsilon_7)$ are consistent with the hypercharge definition

$$Y = \tfrac{2}{3}Q_3 + \tfrac{1}{2}Q_2 + Q_1'. \tag{12}$$

The remaining coefficients $\epsilon_i = \pm 1$ are correlated through the superpotential terms needed to generate masses for quarks and lepton fields; the relevant Yukawa couplings are

$$\mathcal{W} = \lambda_u Q u^c H_u + \lambda_d Q d^c H_d + \lambda_l L H_d e^c \tag{13}$$

and imply the relations $\epsilon_3 = -\epsilon_9, \epsilon_5 = -\epsilon_7$. We may define the baryon number to be $Q_B = \frac{1}{3}Q_C$, while, for the given configuration, the lepton number can be a combination of the form

$$Q_{\mathcal{L}} = a\left(Q_3 + Q_2 + Q_1' - \epsilon_3 \frac{1+a}{a} Q_2'\right) \tag{14}$$

where a is a parameter to be specified. Demanding that the fermion and Higgs fields have the appropriate lepton number, one finds that $a = -\frac{1}{2}, \epsilon_3 = +1$ thus

$$Q_{\mathcal{L}} = -\tfrac{1}{2}(Q_2 + Q_2 + Q_1' + Q_2'). \tag{15}$$

Finally, taking into account all the constraints, it is found that the $\epsilon_{3,5,7,9}$ can be expressed in terms of one parameter only $\epsilon_3 = \epsilon_7 = -\epsilon_5 = -\epsilon_9 = +1$, while the resulting charge assignments are shown in Table III.

Last, the model should also predict a sufficiently suppressed neutrino mass. This may be achieved through a seesaw type mechanism which requires the presence of a right-handed neutrino with both Dirac and Majonana masses. The existence of a Dirac mass term

$$\lambda_l L H_u \nu^c \tag{16}$$

is possible if the RH-neutrino is produced by a string with both ends attached to the same $U(1)$ (bulk) brane with $U(1)$ charges $(0, 0, 0, 2)$ which is part of a vector multiplet as described in [5]. We also note that all dangerous Yukawa terms of the form

[4]For implications of low string scale models see Ref. [18].

TABLE III. The quantum numbers of the SM matter fields for the $N = 2$ brane configuration.

	$SU(3) \times SU(2)$	Q_3	Q_2	Q'_1	Q'_2
Fermions	$Q(3, 2)$	1	-1	0	0
	$u^c(\bar{3}, 1)$	-1	0	0	1
	$d^c(\bar{3}, 1)$	-1	0	1	0
	$L(1, 2)$	0	-1	0	-1
	$e^c(1, 1)$	0	0	1	1
Bosons	$H_u(1, 2)$	0	1	0	-1
	$H_d(1, 2)$	0	1	-1	0

$$\lambda_1 Q d^c L + \lambda_2 u^c d^c d^c + \lambda_3 L L e^c \tag{17}$$

are forbidden by the $U(1)$ symmetries, unless extra singlets generate them at higher order. Such terms can also appear through instanton effects, as it is the case for the ν^c-mass term.

IV. THE TWO-LOOP RENORMALIZATION GROUP ANALYSIS

The bottom-up approach in analyzing SM-like models derived from brane setups reveals that the number of the additional $U(1)$ branes as well as their orientation with respect to the $U(3)$ and $U(2)$ stacks have a significant impact on the determination of the string scale. Up till now, the analysis was restricted to one-loop order. Several issues related to measurements at experimentally accessible energies, however, require a more refined analysis for the various mass scales of the theory. In this section, we will proceed to a two-loop renormalization group calculation in order to get a more accurate value for the string scale as a function of the split SUSY mass, while, in the next section, these new results will be used to determine sensitive quantities such as branching ratios for flavor violating processes for which strict experimental bounds exist.

In the present approach, apart from the electroweak scale M_Z, we assume the existence of two additional mass scales, the string M_S and the split SUSY $\tilde{m}$ scales. The string scale is defined through the gauge couplings relation

$$\frac{1}{\alpha_1} = \frac{n_1}{\alpha_3} + \frac{n_2}{\alpha_2} \tag{18}$$

subject to the ''naturality'' condition $\alpha_2 \leq \alpha_3$ at M_S. This condition ensures that the couplings α_2, α_3 do not meet at a scale lower than the one defined by (17). If $\alpha_2 = \alpha_3$ is realized prior to the condition (17), the scale M_S is then defined at the point where these two couplings meet. For a given D-brane configuration, n_1 and n_2 are expressed in terms of the particular values of k_i, k'_i in (5), and their values are given in the last column of Table I.

In order to define $\tilde{m}$, we assume for simplicity that all scalars acquire a common mass at a scale between the string and the electroweak scale. This scale is identified with $\tilde{m}$, below which only gauginos and higgsinos survive from the SUSY spectrum. All viable models in the context described previously will be considered. We will start with models containing the MSSM spectrum; however, our analysis will be extended to include exotic states like leptoquarks, which *do* arise in certain D-brane constructions.

The 2-loop renormalization group equations for the gauge couplings are given by

$$\frac{d\alpha_i}{dt} = \frac{2b_i\alpha_i^2}{4\pi} + \frac{2\alpha_i^2}{(4\pi)^2}\Bigg[\sum_{j=1}^{3} b_{ij}\alpha_j - \sum_{k=u,d,e} \frac{d_i^k}{4\pi} \mathrm{Tr}(h^{k\dagger}h^k) - d_i^W(\tilde{\alpha}_u + \tilde{\alpha}_d) - d_i^B(\tilde{\alpha}'_u + \tilde{\alpha}'_d)\Bigg] \tag{19}$$

where $\tilde{\alpha}_u$, $\tilde{\alpha}_d$, $\tilde{\alpha}'_u$, and $\tilde{\alpha}'_d$ stand for the gaugino couplings appearing in the split SUSY Lagrangian, α_i $(i = 1, 2, 3)$ are the gauge couplings, and h^k $(k = u, d, e)$ are the Yukawa couplings. Below $\tilde{m}$ the coefficients of Eq. (18) are given by [19]

$$\begin{aligned}
b_i &= \left(\frac{15}{2}, -\frac{7}{6}, -5\right), \qquad b_{ij} = \begin{pmatrix} \frac{104}{9} & 6 & \frac{44}{3} \\ 2 & \frac{106}{3} & 12 \\ \frac{11}{6} & \frac{9}{2} & 22 \end{pmatrix}, \\
d_i^u &= \left(\frac{17}{6}, \frac{3}{2}, 2\right), \qquad d_i^d = \left(\frac{5}{6}, \frac{3}{2}, 2\right), \\
d_i^e &= \left(\frac{5}{2}, \frac{1}{2}, 0\right), \qquad d_i^W = \left(\frac{3}{4}, \frac{11}{4}, 0\right), \\
d_i^B &= \left(\frac{1}{4}, \frac{1}{4}, 0\right).
\end{aligned} \tag{20}$$

Above $\tilde{m}$ we have the usual MSSM spectrum and the coefficients are

$$\begin{aligned}
b_i &= (11, 1, -3), \qquad b_{ij} = \begin{pmatrix} \frac{199}{9} & 9 & \frac{88}{3} \\ 3 & 25 & 24 \\ \frac{11}{3} & 9 & 14 \end{pmatrix}, \\
d_i^u &= \left(\frac{26}{3}, 6, 4\right), \qquad d_i^d = \left(\frac{14}{3}, 6, 4\right), \\
d_i^e &= (6, 2, 0), \qquad d^W = 0, \qquad d^B = 0.
\end{aligned} \tag{21}$$

The proper treatment of the two-loop RGE's for gauge couplings require also the inclusion of the one-loop running for the Yukawa couplings. Thus, the Yukawa coupling RGE's below $\tilde{m}$ are given by

$$\frac{dh^u}{dt} = \frac{h^u}{4\pi}\left(-3\sum_{i=1}^{3} c_i^u\alpha_i + \frac{1}{4\pi}\frac{3}{2}h^{u\dagger}h^u - \frac{1}{4\pi}\frac{3}{2}h^{d\dagger}h^d + \frac{1}{4\pi}T\right), \tag{22}$$

$$\frac{dh^d}{dt} = \frac{h^d}{4\pi}\left(-3\sum_{i=1}^{3} c_i^d \alpha_i - \frac{1}{4\pi}\frac{3}{2}h^{u\dagger}h^u + \frac{1}{4\pi}\frac{3}{2}h^{d\dagger}h^d + \frac{1}{4\pi}T\right), \tag{23}$$

$$\frac{dh^e}{dt} = \frac{h^e}{4\pi}\left(-3\sum_{i=1}^{3} c_i^e \alpha_i + \frac{1}{4\pi}\frac{3}{2}h^{e\dagger}h^e + \frac{1}{4\pi}T\right), \tag{24}$$

where

$$\frac{1}{4\pi}T = \frac{1}{4\pi}\mathrm{Tr}(3h^{u\dagger}h^u + 3h^{d\dagger}h^d + 3h^{e\dagger}h^e) + \frac{3}{2}(\tilde{\alpha}_u + \tilde{\alpha}_d) + \frac{1}{2}(\tilde{\alpha}'_u + \tilde{\alpha}'_d), \tag{25}$$

$$c_i^u = \left(\frac{17}{36}, \frac{3}{4}, \frac{8}{3}\right), \qquad c_i^d = \left(\frac{5}{36}, \frac{3}{4}, \frac{8}{3}\right), \qquad c_i^e = \left(\frac{3}{4}, \frac{3}{4}, 0\right).$$

Above $\tilde{m}$ scale the RGE's are (now h^k is replaced by λ^k)

$$\frac{d\lambda^u}{dt} = \frac{\lambda^u}{4\pi}\left(-2\sum_{i=1}^{3} c_i^u \alpha_i + \frac{1}{4\pi}\lambda^{u\dagger}\lambda^u + \lambda^{d\prime}\lambda^u + \frac{1}{4\pi}3\,\mathrm{Tr}(\lambda^{u\dagger}\lambda^u)\right), \tag{26}$$

$$\frac{d\lambda^d}{dt} = \frac{\lambda^d}{4\pi}\left(-2\sum_{i=1}^{3} c_i^d \alpha_i + \frac{1}{4\pi}3\lambda^{u\dagger}\lambda^u + \frac{1}{4\pi}\,\mathrm{Tr}(3\lambda^{d\dagger}\lambda^d + \lambda^{e\dagger}\lambda^e)\right), \tag{27}$$

$$\frac{d\lambda^e}{dt} = \frac{\lambda^e}{4\pi}\left(-2\sum_{i=1}^{3} c_i^e \alpha_i + \frac{1}{4\pi}3\lambda^{e\dagger}\lambda^e + \frac{1}{4\pi}\,\mathrm{Tr}(3\lambda^{d\dagger}\lambda^d + \lambda^{e\dagger}\lambda^e)\right), \tag{28}$$

where

$$c_i^u = \left(\frac{13}{18}, \frac{3}{2}, \frac{8}{3}\right), \qquad c_i^d = \left(\frac{7}{18}, \frac{3}{2}, \frac{8}{3}\right), \qquad c_i^e = \left(\frac{3}{2}, \frac{3}{2}, 0\right). \tag{29}$$

Finally, the gaugino coupling RGE's are

$$\frac{d\tilde{\alpha}_u}{dt} = \frac{2\tilde{\alpha}_u}{4\pi}\left(-3\sum_{i=1}^{3} C_i \alpha_i + \frac{5}{4}\tilde{\alpha}_u - \frac{1}{2}\tilde{\alpha}_d + \frac{1}{4}\tilde{\alpha}'_u\right) + \frac{2}{4\pi}\sqrt{\tilde{\alpha}_u\tilde{\alpha}_d\tilde{\alpha}'_u\tilde{\alpha}'_d} + \frac{2\tilde{\alpha}_u}{(4\pi)^2}T, \tag{30}$$

$$\frac{d\tilde{\alpha}'_u}{dt} = \frac{2\tilde{\alpha}'_u}{4\pi}(-3\sum_{i=1}^{3} C'_i \alpha_i + \frac{3}{4}\tilde{\alpha}'_u + \frac{3}{2}\tilde{\alpha}'_d + \frac{3}{4}\tilde{\alpha}_u) + 3\frac{2}{4\pi}\sqrt{\tilde{\alpha}_u\tilde{\alpha}_d\tilde{\alpha}'_u\tilde{\alpha}'_d} + \frac{2\tilde{\alpha}'_u}{(4\pi)^2}T, \tag{31}$$

$$\frac{d\tilde{\alpha}_d}{dt} = \frac{2\tilde{\alpha}_d}{4\pi}\left(-3\sum_{i=1}^{3} C_i \alpha_i + \frac{5}{4}\tilde{\alpha}_d - \frac{1}{2}\tilde{\alpha}_u + \frac{1}{4}\tilde{\alpha}'_d\right) + \frac{2}{4\pi}\sqrt{\tilde{\alpha}_u\tilde{\alpha}_d\tilde{\alpha}'_u\tilde{\alpha}'_d} + \frac{2\tilde{\alpha}_d}{(4\pi)^2}T, \tag{32}$$

$$\frac{d\tilde{\alpha}'_d}{dt} = \frac{2\tilde{\alpha}'_d}{4\pi}\left(-3\sum_{i=1}^{3} C'_i \alpha_i + \frac{3}{4}\tilde{\alpha}'_d + \frac{3}{2}\tilde{\alpha}'_u + \frac{3}{4}\tilde{\alpha}_d\right) + 3\frac{2}{4\pi}\sqrt{\tilde{\alpha}_u\tilde{\alpha}_d\tilde{\alpha}'_u\tilde{\alpha}'_d} + \frac{2\tilde{\alpha}'_d}{(4\pi)^2}T, \tag{33}$$

where

$$C_i = \left(\frac{1}{4}, \frac{11}{4}, 0\right), \qquad C'_i = \left(\frac{1}{4}, \frac{3}{4}, 0\right).$$

The matching conditions at $\tilde{m}$ are

$$\tilde{\alpha}_u = \alpha_2 \sin^2\beta, \qquad \tilde{\alpha}_d = \alpha_2 \cos^2\beta, \qquad \tilde{\alpha}'_u = \alpha_1 \sin^2\beta, \qquad \tilde{\alpha}_d = \alpha_1 \cos^2\beta, \qquad h^u = \lambda^{u*}\sin\beta, \qquad h^{d,e} = \lambda^{d,e*}\cos\beta, \tag{34}$$

where $\tan\beta$ is the ratio of the two vacuum expectation values.

In solving the two-loop RGE's for the gauge couplings (α_i, $i = 1, 2, 3$), gaugino couplings (α_u, α_d, α'_u, α'_d),and the Yukawa couplings λ^u and h^u, we followed the bottom-up approach beginning at the scale M_Z where the initial conditions for the gauge and the Yukawa couplings are well known experimentally.[5] The missing initial conditions for the gaugino couplings at M_Z can be determined as follows. First, we construct an exact power series solution for the relevant RGE's. Then, we approximate the truncated power series by means of Pade approximants. The sought initial conditions can be found by solving (34). Finally, we numerically (re)solved the whole system requiring the matching at $\tilde{m}$ to be valid within an error of less than 1%. In the actual running the error was less than 0.4%.

We begin by first considering the case of $SU(3)$ and $SU(2)$ gauge couplings unification i.e., when $\xi = 1$. In this case, $k_Y = n_1 + n_2 = \frac{\alpha_s}{\alpha_1}$ where α_s is the unified gauge coupling at M_S. It can be checked that several models in Table I predict the standard $SU(5)$ normalization $k_Y = 5/3$. In Fig. 2 we plot M_S in (a) and the sum $n_1 + n_2$ in (b) as functions of $\tilde{m}$. The band delimits the $\alpha_3(M_Z)$ experimental uncertainty. The solid lines correspond to the 2-loop running while the dotted ones to the 1-loop running. In (b) we also show the line $n_1 + n_2 = 5/3$. This figure confirms that the condition $a_3 = a_2$ is satisfied for $M_S \sim 10^{16}$ GeV, regardless of the number of $U(1)$ branes added in the configuration, provided that the specific setup ensures that $k_Y = \frac{5}{3}$.

[5] We have taken into account the running of the Yukawa coupling from m_{top} to M_Z.

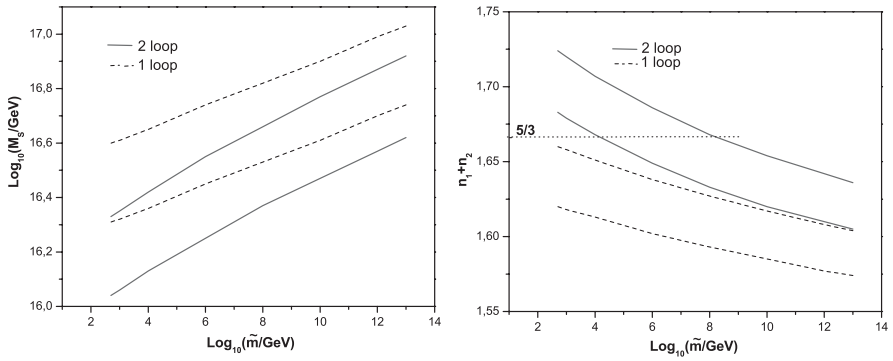

FIG. 2. The M_S scale. (a) and the sum $n_1 + n_2$; (b) as a function of $\log_{10}\tilde{m}$ for the case where $\alpha_3 = \alpha_2$ at M_S. The bands correspond to the strong coupling experimental error at M_Z. The solid lines correspond to 2-loop running while the dotted ones to 1-loop.

The M_S scale found here is expected to be higher than the corresponding unification scale of the MSSM. This is due to the presence, in the split case and below $\tilde{m}$, of extra degrees of freedom (gauginos and higgsinos) which modify the β functions. The width of the band which corresponds to the strong coupling experimental error at M_Z corresponds almost to a factor of 2 in the M_S scale. This is not at all surprising, since simple calculations in 1-loop approximation show that

$$\ln M_S = \ln\tilde{m} + \left(\frac{1}{\alpha_2(M_Z)} - \frac{1}{\alpha_3(M_Z)}\right)\frac{2\pi}{b_2^S - b_3^S} - \frac{b_2^{SP} - b_3^{SP}}{b_2^S - b_3^S}(\ln\tilde{m} - \ln M_Z)$$

where the superscript S (SP) to the b coefficients corresponds to the SUSY (split SUSY) case. The difference in $\ln M_S$, due to the strong coupling error and for constant m is given by

$$\frac{\Delta^{\text{strong}} M_S}{M_S} = \Delta^{\text{strong}}\left(\frac{1}{\alpha_2(M_Z)} - \frac{1}{\alpha_3(M_Z)}\right)\frac{2\pi}{b_2^S - b_3^S} = \sim 0.666.$$

The correlation of the string and split SUSY scales for different values of k_Y, can be seen in Fig. 3 where we plot M_S as a function of k_Y. It can be readily seen that the M_S value is not very sensitive to the value of k_Y.

Next, relaxing the requirement of $SU(3)$ and $SU(2)$ gauge coupling unification, we calculate M_S for all models that satisfy the relation $n_1 + n_2 = 5/3$ as a function of $\tilde{m}$. Since the equality of α_2 and α_3 at M_S is no longer required, different models evolve differently. The results are depicted in Fig. 4. It is interesting to realize that all the curves have one common point. In other words, there exists a singled out $\tilde{m}$ value that gives the same M_{string} for all models in this class. This is expected as we have seen in our first approach and in Fig. 3: If we choose a specific $\tilde{m}$ scale we can satisfy Eq. (18) at a scale M_S with the additional requirement that at this scale $\alpha_3 = \alpha_2$. All models corresponding to a given $n_1 + n_2$ behave similarly. This behavior is independent of 1-loop or 2-loop running, although these special points are different [see Fig. 4(b)]. Notice also the big difference (6 orders of magnitude) in the value of $\tilde{m}$ between the corresponding meeting point of 1- and 2-loop running although the difference in M_S is much smaller. This point is also made clear in Fig. 2(b), where the curves meet the $5/3$ value at very low $\tilde{m}$.

In Fig. 5 we show for the sake of completeness, the corresponding graph for two more models, namely, (8/3, 1) and (14/3, 1). The values for both M_S and $\tilde{m}$ are now found to be much smaller than before.

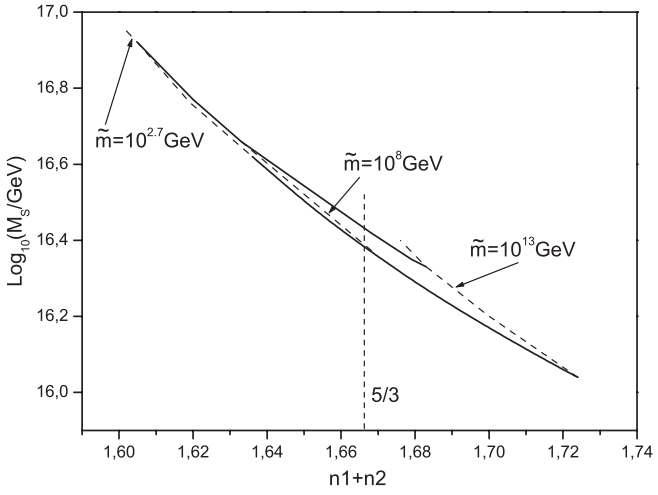

FIG. 3. The M_S scale as a function of $n_1 + n_2$. The two curves correspond to the $a_3(M_Z)$ experimental uncertainty. Curves of constant $\tilde{m}$ are shown for the values $10^{2.7}$, 10^8, and 10^{13} GeV.

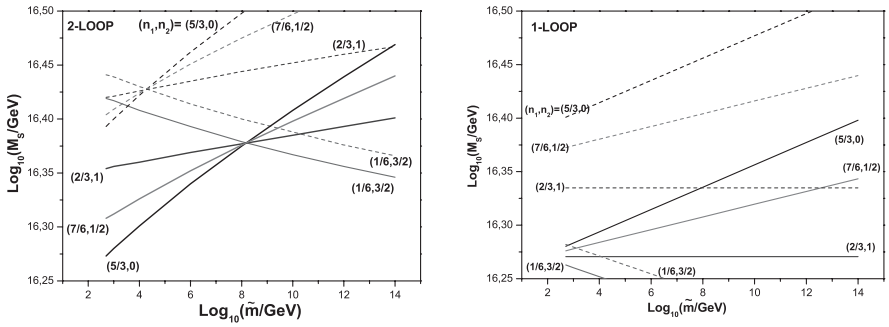

FIG. 4. The M_S scale as a function of $\tilde{m}$, for 2-loop running (a) and 1-loop running (b), for the models having $n_1 + n_2 = 5/3$. Continuous lines correspond to the lower value of $\alpha_3(M_Z)$ while dotted ones to the higher one.

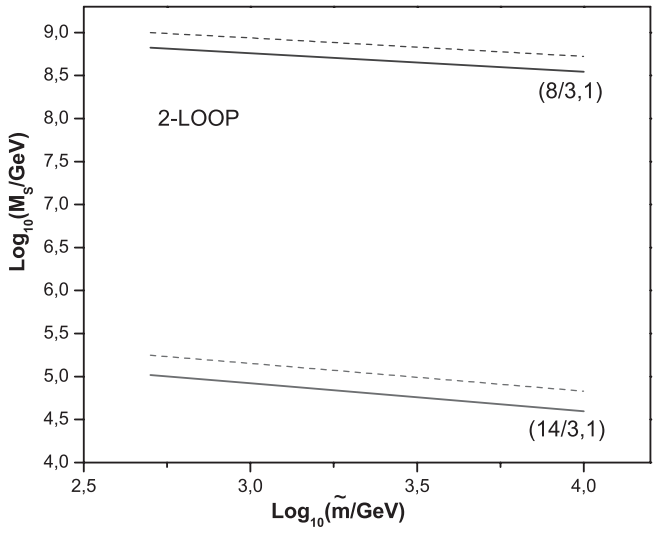

FIG. 5. The M_S scale as a function of $\tilde{m}$, for 2-loop running for the models with $(8/3, 1)$ and $(14/3, 1)$. Continuous lines correspond to the lower value of $\alpha_3(M_Z)$ while dotted ones to the higher one.

V. MIRRORS

As mentioned previously, D-brane constructions include states with the quantum numbers of leptoquarks. Such cases have already been analyzed in the context of conformal field theory orientifolds models. Here, we will pick up the 32 models presented in [17] which also have the advantage of inducing neutrino Majorana masses through instanton effects. The extra particles of these models consist of mirror states having the same quantum numbers (under the SM gauge group) as the standard ones, with the exception of singlet neutrinos and d-like leptoquarks, i.e. states with the quantum numbers of d-quarks carrying both lepton and baryon number. Four brane-stack configurations are considered in the above construction, two of them carrying the $SU(3)$ and the $SU(2)$, with 2 more providing either a $U(1)$ and an $O(2)$ or two $U(1)$ factors. A similar analysis can also be carried out for the five brane-stack scenario discussed in the present work.

The above 32 models correspond to only 12 distinct spectra with the exotic states shown in Table IV. The doublet and the singlet quarks are denoted by Q, U, and D, respectively; the doublet and the singlet leptons are L and E; N are the right-handed neutrinos; Y stands for the leptoquarks; and finally, H represents the Higgs fields. Note that in these models the minimum number of RH neutrinos required is 3 (to avoid the cubic anomaly); however, since these are singlets under the SM gauge group, they do not contribute to the running of the couplings.

We will now repeat the renormalization group analysis for these models, including also the exotic states. Starting again from the known initial values of the three SM couplings at M_Z, we determine, for each of the above models, the pair $(\tilde{m}, M_S)$ subject to the "unification" condition (18) at M_S. Above $\tilde{m}$ we have the complete MSSM spectrum enriched by the extra mirrors appearing in Table IV. Below $\tilde{m}$, we have split SUSY containing extra quarks, leptons, leptoquarks, and higgsinos, while we keep one Higgs doublet only as in the original split scenario. Since our group is the SM one, no extra gauginos appear.

In Fig. 6 we plot the one-loop results for the 12 models together with the case of no extra mirrors (thick line) and for (n_1, n_2) equal to $(14/3, 1)$ and $(8/3, 1)$, respectively.

TABLE IV. The 12 possible configurations of extra mirror content

Model	Q	U	D	L	E	N	Y	H
1	0	0	0	0	2	3	2	16
2	0	0	0	0	2	3	6	16
3	0	0	0	2	2	3	6	8
4	0	0	0	2	2	3	6	24
5	0	0	0	6	2	3	2	8
6	0	0	0	6	2	3	2	24
7	2	0	0	0	2	3	2	16
8	2	0	0	0	2	3	6	16
9	4	0	0	2	2	3	2	8
10	4	0	0	2	2	3	2	24
11	4	0	0	6	2	3	6	8
12	4	0	0	6	2	3	6	24

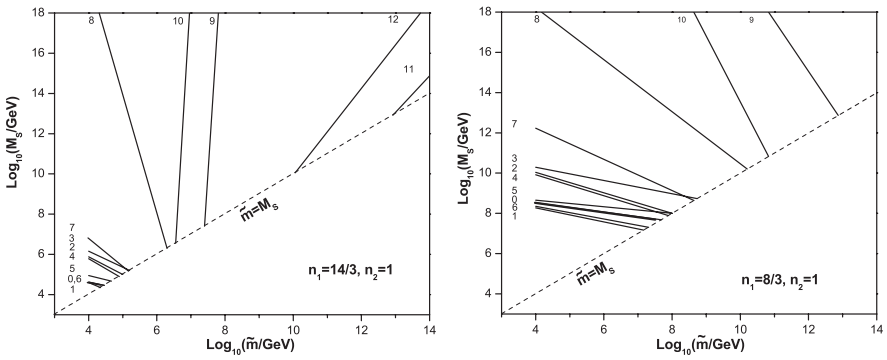

FIG. 6. Plots of M_S vs $\tilde{m}$ for the 12 models appearing in Table IV and the two cases of the pair (n_1, n_2). The thicker line corresponds to the case with no mirrors (0 model) while the label corresponds to the model as in Table IV.

The allowed region lies above the $\tilde{m} = M_S$ line. The emerging picture seems to favor higher M_S values as compared to the minimal cases discussed previously. Notice that in models 9 and 10, $\tilde{m}$ is almost fixed ($10^{6.5}$ and $10^{7.5}$) while M_{string} varies along the whole (acceptable) range.

Some comments are in order here. In Fig. 6(a), the depicted models can be grouped in three distinctive classes: (i) In the low M_S class, the higher $\tilde{m}$ the lower M_S. (ii) In the class with high M_S the tendency is reversed. (iii) The third class has almost constant $\tilde{m}$ while M_S varies along the whole (acceptable) range. In Fig. 6(b), the majority of the models show that M_S is less sensitive against the variation of $\tilde{m}$. This rather peculiar behavior can be easily explained if we recall Eq. (7) written in the form

$$\ln\left[\frac{M_S}{M_Z}\right] = a \ln\left[\frac{\tilde{m}}{M_Z}\right] + b\cdot$$

In models of the first class $a < 0$. In class (ii) $a > 0$ and M_S increases with $\tilde{m}$. Finally, for models in (iii) a is very large and M_S is almost independent of $\tilde{m}$.

VI. THE LEPTON FLAVOR VIOLATING PROCESS $\mu \to e\gamma$

One of the most important flavor violating rare processes present in all models with flavor mixing in the Yukawa sector is the decay of the muon to an electron-photon pair. In ordinary supersymmetric theories, this exotic process is usually suppressed by powers of the supersymmetry breaking scale which is of the order of 1 TeV at the most [20,21]. If the scalar partners involved in the process are nonuniversal, hard violations of the lepton number conservation that exceed the present experimental limits are expected. Even in the case of universal masses at the unification scale, renormalization effects result in mass splitting and important mixing effects at low energies. Although there is a certain degree of ambiguity due to the unknown mixing details in lepton and slepton mass matrices in the calculation of the branching ratios, a significant portion of the universal gaugino mass–universal scalar mass parameter space $(m_{1/2}, m_0)$ is excluded in ordinary supersymmetric models. In the present analysis, we examine the conditions for accessibility of this interesting decay in the context of the D-brane constructions discussed above.

In split SUSY, the scale of the slepton masses is set by the $\tilde{m}$ scale which is considered to be much higher than the TeV ordinary SUSY scale. The renormalization group analysis of the generic D-brane constructions has shown, however, that in several cases the $\tilde{m}$ can be as low as a few TeV. Graphs for $\mu \to e\gamma$ are mediated by the above scalars. It is worth exploring whether in some of the above models these exotic reactions could be observed in future experiments. The branching ratio of the $\mu \to e\gamma$ process is given by [20,21]

$$\text{BR}(\mu \to e\gamma) = \frac{48\pi^3\alpha}{G_F^2}(|A_2^L|^2 + |A_2^R|^2)$$

where

$$A_2^L = A_2^{(n)L} + A_2^{(c)L} \quad \text{and} \quad A_2^R = A_2^{(n)R} + A_2^{(c)R}\cdot$$

The superscript n (c) of the amplitudes A corresponds to the neutralino (chargino) exchange contribution and L (R) to the left- (right-) handed incoming lepton. The amplitudes are given by the relations

$$A_2^{(n)L} = \frac{1}{32\pi^2}\frac{1}{\tilde{m}_{\tilde{l}_X}^2}\left[N_{1AX}^{L(l)}N_{2AX}^{L(l)*}f_1(r) + N_{1AX}^{L(l)}N_{2AX}^{R(l)*}\frac{M_{\tilde{\chi}_A^0}}{m_\mu}f_2(r)\right], \tag{35}$$

$$A_2^{(c)L} = -\frac{1}{32\pi^2}\frac{1}{\tilde{m}_{\tilde{\nu}_X}^2}\left[C_{1AX}^{L(l)}C_{2AX}^{L(l)*}f_3(r') + C_{1AX}^{L(l)}C_{2AX}^{R(l)*}\frac{M_{\tilde{\chi}_A^-}}{m_\mu}f_4(r')\right], \tag{36}$$

$$A_2^{(n)R} = A_2^{(n)L}|_{L\leftrightarrow R} \quad \text{and} \quad A_2^{(c)R} = A_2^{(c)L}|_{L\leftrightarrow R}. \tag{37}$$

We are working with the mass eigenstates so all matrices rotating from the weak to the mass eigenstates are moved to the vertices. The neutral amplitude involves the neutralinos and the charged sleptons with corresponding masses $M_{\tilde{\chi}_A^0}$ $(A = 1, \ldots, 4)$ and $\tilde{m}_{\tilde{l}_X}$ $(X = 1, \ldots, 6)$ while m_μ is the mass of the decaying muon. The charged amplitude involves the charginos and sneutrinos with corresponding masses $M_{\tilde{\chi}_A^-}$ $(A = 1, 2)$ and $\tilde{m}_{\tilde{\nu}_X}$ $(X = 1, 2, 3)$. The matrices $N_{iAX}^{L(l)}$ and $N_{iAX}^{R(l)}$ involve both the neutralino and the slepton rotating matrices ($i = 1$ for the electron and $i = 2$ for the muon) and are given by

$$N_{iAX}^{R(l)} = -\frac{g_2}{\sqrt{2}}\Big\{[-(O_N)_{A2} - (O_N)_{A1}\tan\theta_W]U_{Xi}^l + \frac{m_i}{m_W\cos\beta}(O_N)_{A3}U_{X(i+3)}^l\Big\},$$

$$N_{iAX}^{L(l)} = -\frac{g_2}{\sqrt{2}}\Big\{\frac{m_i}{m_W\cos\beta}(O_N)_{A3}U_{Xi}^l + 2(O_N)_{A1} \times \tan\theta_W U_{X(i+3)}^l\Big\}.$$

The matrices O_N rotate the neutralinos while U^l rotate the charged sleptons. Finally, m_i is the lepton mass ($m_1 = m_e$, $m_2 = m_\mu$).

The matrices $C_{iAX}^{L(l)}$ and $C_{iAX}^{L(l)}$ (again $i = 1$ for the electron and $i = 2$ for the muon) involve both the chargino (O_L and O_R) and the sneutrino (U^ν) rotating matrices and they are given by

$$C_{iAX}^{R(l)} = -g_2(O_R)_{A1}U_{Xi}^\nu,$$

$$C_{iAX}^{L(l)} = g_2\frac{m_i}{\sqrt{2}m_W\cos\beta}(O_L)_{A2}U_{Xi}^\nu.$$

Finally, the f functions appearing in Eqs. (35) and (36) are

$$f_1(r) = \frac{1}{6(1-r)^4}(1 - 6r + 3r^2 + 2r^3 - 6r^2\ln(r)),$$

$$f_2(r) = \frac{1}{(1-r)^3}(1 - r^2 + 2r\ln(r)),$$

$$f_3(r') = \frac{1}{6(1-r')^4}(2 + 3r' - 6r'^2 + r'^3 + 6r'\ln(r')),$$

$$f_4(r') = \frac{1}{(1-r)^3}(-3 + 4r' - r'^2 - 2\ln(r'))$$

where $r = \dfrac{M_{\tilde{\chi}_A^0}^2}{\tilde{m}_{\tilde{l}_X}^2}$ and $r' = \dfrac{M_{\tilde{\chi}_A^-}^2}{\tilde{m}_{\tilde{\nu}_X}^2}$.

In estimating the $\mu \to e\gamma$ branching ratio and in order not to complicate our analysis we have ignored the neutralino and the chargino mixing[6] (i.e. the O_L, O_R, and O_N matrices are the identity matrix) and have dropped terms proportional to the mass of the leptons. Therefore, we are left with the U^l and U^ν matrices.

The 6×6 charged slepton matrix is given by

$$\begin{pmatrix} m_{LL}^2 & m_{LR}^2 \\ m_{RL}^2 & m_{RR}^2 \end{pmatrix} \tag{38}$$

where each entry is a 3×3 matrix with an obvious notation and [22]

$$m_{LL}^2 = (\tilde{m}_l^\delta)^2 + \delta m_N^2 + m_l^2 + M_Z^2\Big(\frac{1}{2} - \sin^2\theta_W\Big)\cos2\beta, \tag{39}$$

$$m_{RR}^2 = (\tilde{m}_{\tilde{e}_R}^\delta)^2 + m_l^2 - M_Z^2\sin^2\theta_W\cos2\beta, \tag{40}$$

$$m_{RL}^2 = (A_e^\delta + \delta A_e + \mu\tan\beta)m_l, \tag{41}$$

$$m_{LR}^2 = m_{RL}^{2\dagger}. \tag{42}$$

The superscript δ denotes the diagonal part of the corresponding 3×3 matrix and we have assumed universal soft masses, so that $(\tilde{m}_l^\delta)^2 = (\tilde{m}_{\tilde{e}_R}^\delta)^2 = \text{Diagonal}\,(m_0, m_0, m_0)$ where in our case, $m_0 = \tilde{m}$. Also, $A_e^\delta = \text{Diagonal}\,(A_0, A_0, A_0)$ with $A_0 = -1.5m_0$. The terms δm_N^2 and δA_e stand for the off-diagonal matrices which arise because of the nondiagonal Yukawa coupling λ_D (in the basis where the lepton matrix is diagonal) appearing in the term which gives mass to the neutrino through the superpotential term $N^c\lambda_D l H_2$ and in the trilinear coupling of the potential correspondingly. The sneutrino reduced 3×3 matrix ([22]) is given by

$$\tilde{m}_{\tilde{\nu}}^2 = (\tilde{m}_{\tilde{l}}^\delta)^2 + \delta m_N^2 + \frac{1}{2}M_Z^2\cos2\beta. \tag{43}$$

The off-diagonal matrices δm_N^2 and δA_e are evaluated in [22] for the region of $\tan\beta = 3 - 14$. Having determined the mass matrices for the charged sleptons and the sneutrino, we can find the matrices U^l and U^ν which rotate to the corresponding mass eigenstates and, therefore, proceed to the evaluation of the desired branching ratio. In Fig. 7 we show the branching ratio (BR) as a function of $\tilde{m}$ for the above region of $\tan\beta$ and for $\mu = 200$–800 GeV. We clearly see that for the present experimental BR bound (10^{-12}), $\mu \to e\gamma$ could be observed in models allowing $\tilde{m}$ around 1.5 TeV (for the evaluation of the BR we have assumed a universal gaugino mass of 200 GeV, since we run our RGE's with the split SUSY regime active down to the weak scale).

[6]Actually, an explicit calculation for the models under consideration shows that inclusion of the neutralino and chargino mixing matrices modifies the branching ratio by less that 10%.

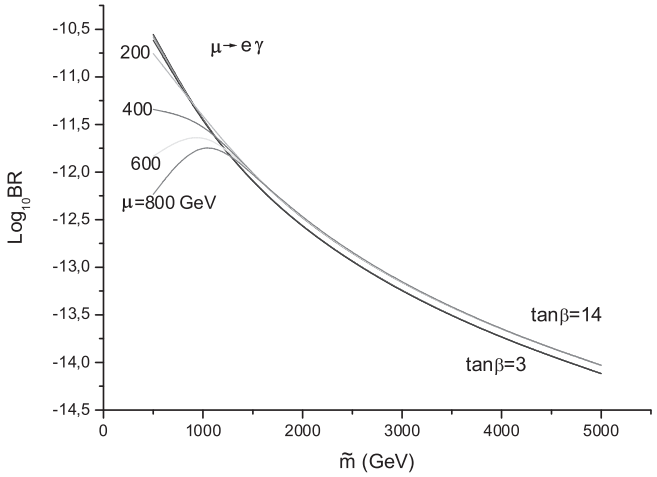

FIG. 7. The (logarithm of the) branching ratio of $\mu \to e\gamma$ as a function of $\tilde{m}$ for $\tan\beta = 3$ and 14 and for $\mu = 200$, 400, 600, 800 GeV.

From the renormalization group analysis of the previous section, we can check that for a wide class of D-brane constructions, the split-supersymmetric scale ranges from 1 TeV up to values as high as 10^{13} GeV. The above reaction could in principle be observed in the present day experiments for the lower marginal values of the split SUSY scale as it can also be seen from Figs. 2 and 3. However, if we stick to cases where we have $a_3 = a_2$ unification at M_S, the $U(1)_Y$ normalization constant k_Y is found to be around the standard value $\frac{5}{3}$. Then, from Fig. 3 we observe that $\tilde{m} \sim 10^8$ GeV; therefore, the branching ratio is significantly suppressed and lies far beyond the capabilities of even future experiments.

On the other hand, the observability prospects of this reaction are different in models implying low string scale, since the split scale $\tilde{m}$ cannot be higher than $\tilde{m} \leq M_S \sim 5$ TeV. For $\tilde{m} \sim 5$ TeV, the $\mu \to e\gamma$ branching ratio is $\mathrm{BR}_{\mu\to e\gamma} \sim 10^{-14}$, a number that could in principle be checked in future experiments. Thus, for this particular class of D-brane constructions, muon number violating reactions can probe the whole $\tilde{m}$ region.

VII. CONCLUSIONS

D-branes brought profound changes in our approach to model building. In the present work, we presented the simplest D-brane extensions of the standard model based on configurations with gauge symmetry of the form $U(3) \times U(2) \times U(1)^P$ with $P \leq 3$. Exploring the different brane-stack orientations in the higher dimensional space as well as the various hypercharge embeddings consistent with the SM particle spectrum, we managed to obtain a complete classification of the SM variants that arise in this context. We addressed several phenomenological issues affecting the viability of these constructions. These issues were examined in the context of split-supersymmetric spectrum which has been shown to be a natural possibility in a wide class of D-brane constructions. This way, we extended previous investigations on the correlation between the string scale and the split supersymmetry breaking scale, incorporating two-loop effects. The calculations show a significant change on the split supersymmetry breaking scale as compared to the one-loop results, while the string scale for several interesting cases is only moderately affected. The analysis was further extended to nonminimal cases that include leptoquark and mirror states. Yukawa terms providing masses to the SM fields were calculated, while the problem of incorporating the right-handed neutrino mass through instanton effects was also mentioned. Finally, we presented a detailed discussion on the possible observability of the $\mu \to e\gamma$ flavor violating decay in the present and future experiments.

ACKNOWLEDGMENTS

The work is partially supported by the EU Grant No. MRTN-CT-2004-503369.

[1] J. Polchinski, Phys. Rev. Lett. **75**, 4724 (1995).
[2] R. Blumenhagen, M. Cvetic, P. Langacker, and G. Shiu, Annu. Rev. Nucl. Part. Sci. **55**, 71 (2005).
[3] R. Blumenhagen, B. Kors, D. Lust, and S. Stieberger, Phys. Rep. **445**, 1 (2007).
[4] I. Antoniadis, E. Kiritsis, and T. Tomaras, Fortschr. Phys. **49**, 573 (2001).
[5] I. Antoniadis, E. Kiritsis, J. Rizos, and T. N. Tomaras, Nucl. Phys. **B660**, 81 (2003).
[6] D. V. Gioutsos, G. K. Leontaris, and J. Rizos, Eur. Phys. J. C **45**, 241 (2006).
[7] P. Anastasopoulos, T. P. T. Dijkstra, E. Kiritsis, and A. N. Schellekens, Nucl. Phys. **B759**, 83 (2006).
[8] D. V. Gioutsos, G. K. Leontaris, and A. Psallidas, Phys. Rev. D **74**, 075007 (2006).
[9] R. Blumenhagen, L. Goerlich, B. Kors, and D. Lust, J. High Energy Phys. 10 (2000) 006.
[10] G. Aldazabal, S. Franco, L. E. Ibanez, R. Rabadan, and A. M. Uranga, J. High Energy Phys. 02 (2001) 047.
[11] E. Kiritsis, Fortschr. Phys. **52**, 200 (2004); Phys. Rep. **421**, 105 (2005); **429**, 121(E) (2006).
[12] N. Arkani-Hamed and S. Dimopoulos, J. High Energy Phys. 06 (2005) 073.
[13] T. Gherghetta and A. Pomarol, Phys. Rev. D **67**, 085018 (2003).
[14] I. Antoniadis and S. Dimopoulos, Nucl. Phys. **B715**, 120

(2005).

[15] D. Cremades, L. E. Ibanez, and F. Marchesano, J. High Energy Phys. 07 (2003) 038.

[16] R. Blumenhagen, M. Cvetic, and T. Weigand, Nucl. Phys. **B771**, 113 (2007); L. E. Ibanez and A. M. Uranga, J. High Energy Phys. 03 (2007) 052; M. Cvetic, R. Richter, and T. Weigand, Phys. Rev. D **76**, 086002 (2007).

[17] L. E. Ibanez, A. N. Schellekens, and A. M. Uranga, J. High Energy Phys. 06 (2007) 011.

[18] V. Barger, P. Langacker, and G. Shaughnessy, New J. Phys. **9**, 333 (2007).

[19] G. F. Giudice and A. Romanino, Nucl. Phys. **B699**, 65 (2004); **706**, B65(E) (2005).

[20] J. Hisano, T. Moroi, K. Tobe, and M. Yamaguchi, Phys. Rev. D **53**, 2442 (1996); J. Hisano and D. Nomura, Phys. Rev. D **59**, 116005 (1999); J. A. Casas and A. Ibarra, Nucl. Phys. **B618**, 171 (2001).

[21] J. R. Ellis, M. E. Gomez, G. K. Leontaris, S. Lola, and D. V. Nanopoulos, Eur. Phys. J. C **14**, 319 (2000); G. K. Leontaris and N. D. Tracas, Phys. Lett. B **431**, 90 (1998); T. Kosmas, G. K. Leontaris, and J. D. Vergados, Phys. Lett. B **219**, 457 (1989).

[22] M. E. Gomez, G. K. Leontaris, S. Lola, and J. D. Vergados, Phys. Rev. D **59**, 116009 (1999).